Plio-Pleistocene Establishment of Irtysh River in Junggar, Northwest China: Implications for Siberian-Arctic River System Evolution and Resulting Climate Impact

Yan Ma[1*], Dewen Zheng[2], Huiping Zhang[1], Jianzhang Pang[1], Weitao Wang[3], Yizhou Wang[1], Ying Wu[1], Huaiyu He[4], Finlay M. Stuart[5] and Sheng Xu[6]

[1] *State Key Laboratory of Earthquake Dynamics, Institute of Geology, China Earthquake Administration, Beijing, 100029, China*

[2] *State Key Laboratory of Isotope Geochemistry, Guangzhou Institute of Geochemistry, Chinese Academy of Sciences, Guangzhou, 510640, China*

[3] *School of Earth Sciences and Engineering, Sun Yat-Sen University, Guangzhou, 510275, China*

[4] *State Key Laboratory of Lithospheric Evolution, Institute of Geology and Geophysics, Chinese Academy of Sciences, Beijing, 100029, China*

[5] *Isotope Geosciences Unit, Scottish Universities Environmental Research Centre (SUERC), East Kilbride, G75 0QF, UK*

[6] *Institute of Surface-Earth System Science, Tianjin University, Tianjin, 300072, China*

[*]Corresponding author.

E-mail address: mayan82634@hotmail.com

Phone number: (86) 13641123884

Present address: State Key Laboratory of Earthquake Dynamics, Institute of Geology, China Earthquake Administration, Yard No.1jia, Hua Yan Li, Chaoyang District, Beijing, 100029, China

Key Points:

- We have constrained the establishment of a major Siberian river—the Irtysh River—to ca. 2.8 Ma by a combination of ^{21}Ne and ^{26}Al/^{10}Be
- The timing of the Irtysh's establishment provides radioisotopic evidence for a geologically young Siberian-Arctic river system
- This work supports a profound impact of Siberian freshwater input to Arctic on Northern Hemisphere ice-sheet expansions during late Pliocene

Abstract

The influence of Siberian freshwater input to the Arctic Ocean on Northern Hemisphere ice-sheet expansions remains poorly known due to the incomplete geologic record of Siberian-Arctic river systems during the late Pliocene. The Irtysh River is a major Siberian river, rising from the Altay Mountains, northwestern China, and flowing 4282 km before joining the Ob River. Here, we present new field evidence and chronological data from a combination of cosmogenic ^{21}Ne and $^{26}Al/^{10}Be$ measurements that constrain the establishment of the Irtysh River to ca. $2.77^{+0.39}/_{-0.33}$ Ma. These first quantitative chronological results, together with previous sedimentological, geomorphological, and geochemical evidence, support a young Siberian-Arctic river system. Its coincidence with the late Pliocene ice-sheet expansions in the Northern Hemisphere implies a profound impact of Siberian freshwater input to the Arctic on the major ice advances that significantly affected global oceanographic and climatic systems.

Plain Language Summary

Siberian rivers presently contribute ~80% of total river discharge to the Arctic Ocean, which has a remarkable effect on decreasing ocean surface salinity and promoting rapid ice-sheet expansions by a series of ice-albedo feedbacks. Although the Siberian-Arctic river system is thought to postdate the late Pliocene on the basis of sedimentological, geomorphological, and geochemical evidence, the profound impact of Siberian freshwater input on the late Pliocene ice-sheet expansions in Northern Hemisphere remains speculative due to lack of precise chronological constraints on its formation. The Irtysh River is a major Siberian-Arctic river, rising from the Altay Mountains in northwest China and flowing ~4282 km before merging with Ob River. In this work, we present new field evidence and chronological data from cosmogenic ^{21}Ne and $^{26}Al/^{10}Be$ that constrain the establishment of the Irtysh River to ca. 2.8 Ma. The timing of its establishment is consistent with previous studies, and supports a young age for Siberian-Arctic rivers. The coincidence of Arctic river formation in Siberia with a major ice advance in the Northern Hemisphere implies a profound impact of Siberian freshwater input to the Arctic on the late Pliocene ice-sheet expansions that affected global oceanographic and climatic systems.

1 Introduction

After a long-term progressive cooling during the late Pliocene, a major intensification of the Northern Hemisphere glaciation began ~2.7 My ago, when the late Pliocene cooling culminated (Jansen et al., 1988; Lisiecki & Raymo, 2005; Ruddiman & Raymo, 1988; Shackleton et al., 1984). Numerous models have been proposed for this rapid glacial expansion, with many inferring a tectonic influence, such as the closure of the Central American seaway that changed the ocean thermohaline circulation and enhanced moisture at high latitudes (Haug et al., 2001), upliftment of the Himalayas that altered the atmospheric circulation (Raymo et al., 1988) and enhanced chemical weathering to deplete the atmospheric CO_2 level (Raymo & Ruddiman, 1992), and the late Neogene deformation of central Asia (De Grave & van den Haute, 2002; Jolivet et al., 2009; Vassallo et al., 2007) that led to the reorganization of Siberian rivers toward the Arctic (Wang, 2004). Non-tectonic mechanisms, such as orbitally-driven variations in insolation, have also been proposed (Maslin et al., 1998). No matter which mechanism is proven to be more reasonable, these tectonically-driven paleooceanographic and paleotopographic changes brought global cooling to a critical threshold.

Siberian rivers contribute ~80% of the total river discharge (3,300 km^3/a) to the Arctic Ocean (Stein, 2000) and have a remarkable effect on Arctic surface circulation. Three major rivers (Fig. 1a), namely, Yenisey (620 km^3/a), Lena (525 km^3/a), and Ob (429 km^3/a), originating in the central Asian plateau, supply more than half of the annual Arctic freshwater runoff (Aagaard & Carmack, 1989; Gordeev et al., 1996). The formation of Arctic rivers in Siberia during the late Pliocene, accompanied by the enhanced moisture transported to northern Eurasia by the westerlies after the closure of the Central American seaway, likely played a key role in delivering freshwater to the Arctic Ocean that triggered ice-sheet expansion, because the abruptly enhanced freshening of

Arctic waters decreased ocean surface salinity and favored sea ice formation. This, in turn, created a series of positive ice-albedo feedbacks and promoted rapid ice-sheet expansion (e.g., Knies et al., 2014; Moran et al., 2006; Zachos et al., 2001).

However, the profound impact of Siberian freshwater input to the Arctic Ocean on the late Pliocene Northern Hemisphere ice-sheet expansions remains speculative because of the lack of precise chronological data on the river system's establishment. Sedimentological, geomorphological, and geochemical studies in Siberia and the Arctic Ocean have provided evidence of a late Pliocene Siberian-Arctic river system. According to stratigraphic correlation, the paleovalleys incised on the western Siberian shelf adjacent to the Ob and Yenisey gulfs and those found along the lower reaches of the Lena River (Fig. 1a) are of late Pliocene–Pleistocene age (Alekseev & Drouchite, 2004; Milanovsky, 2008; Wang, 2004). An abrupt positive change in ε_{Nd} from −8 to −6 (Haley et al., 2007) during the late Pliocene–early Pleistocene period recorded in Arctic drilling cores (Backman et al., 2008) suggests the formation of the Yenisey River that drains the Siberian flood basalts (Fig. 1a), which is the exclusive source of radiogenic Nd (ε_{Nd}: 0–+2.5; Sharma et al., 1991) to the Arctic.

The Irtysh River, originating in the Altay Mountains in northwest China and flowing approximately 4282 km before merging with the Ob River, is a major Siberian-Arctic river (Fig. 1a). It drains a basin of 1.6×10^6 km^2, with a mean annual discharge of 99.8 km^3/a (Gordeev et al., 2004; Huang et al., 2012). Previous sedimentological studies in Junggar Basin, northwest China, revealed that the ancestral Irtysh River was an inland river in Junggar until at least ~6 Ma (Li et al., 2020; Yan & Xia, 1962). As it is a major Siberian river, timing the establishment of the Irtysh River may provide a chronological constraint on the large-scale reorganization of the Siberian drainage system that formed modern Arctic rivers.

In this work, we report a new stratigraphic investigation throughout the Junggar Basin and chronological results of Pliocene alluvial deposits in the region from a combination of cosmogenic ^{21}Ne and $^{26}Al/^{10}Be$ to reconstruct the evolution of the Irtysh River, clarify its implication on the formation of Siberian-Arctic river system, and assess the importance of Siberian rivers in late-Pliocene ice-sheet expansions.

2 Study area

Our study area is in central Asia (Fig. 1a), shielded from the monsoonal influence of India and the northern Pacific Ocean by the Tibetan Plateau. Westerly moisture transport dominates regional precipitation in this region (Caves et al., 2015; Guo et al., 2002; Tian et al., 2001; Wang, 1990). Approximately 1000 km away, Lake Baikal, located in the southern Siberia (Fig. 1a), has preserved continuous terrestrial records of late-Pliocene regional paleoclimate changes in central Asia (Antipina et al., 2001; Kuzmin et al., 2000; Kuzmin et al., 2003; Williams et al., 1997). Sharp drop in diatom abundance and rise in dense glacial clay in lake sediments, as well as the pollen-based temperature and precipitation reconstructions (Fig. 1b) indicate intensive terrestrial glacial expansion accompanying the abrupt cooling in central Asia and increasing moisture delivery to the Eurasian continent at this time.

The Junggar Basin, with an area of 380,000 km^2, is located in northwest China and is separated from the Altay Mountains to the northeast by the NW-trending Ertix fault zone (Fig. 1c). Limited deformation of the Altay Mountains occurred in the early Cenozoic before the activity of the Fuyun fault that began during the early Miocene (Fig. 1c) (Xu et al., 2015; Yuan et al., 2006); the Fuyun fault is still active (Klinger et al., 2011). Cenozoic strata are mainly exposed in the northern part of the Junggar Basin, and those of late Oligocene–Miocene ages are dominated by alternating fluvial and aeolian facies deposits (Sun et al., 2010), indicating that the regional environment has changed frequently since the late Oligocene.

The Irtysh River is the only exorheic river developed in the Junggar Basin (Fig. 1c), and all of its tributaries are sourced from the glaciers on the southwestern slopes of the Altay Mountains. After forming a northwest-flowing trunk stream in the Junggar, it flows west across Kazakhstan via Lake Zaysan, through the western Siberian Plain, and finally empties into the Arctic Ocean. Previous sedimentological studies have revealed that the ancestral Irtysh River was a series of inland rivers rising from the Altay Mountains, flowing southward into a paleolake in the Junggar Basin before ~6 Ma (Li et al., 2020).

3 Materials and methods

3.1 Extent of Pliocene Junggar paleolake

To reconstruct the Pliocene paleolake in the Junggar Basin, we conducted a detailed investigation of lacustrine deposits in the basin, which are exposed only in a few outcrops marked in Fig. 2a. In the outcrop at the northwestern margin of the Junggar (Site α, Fig. 2b), 20-m thick yellowish mudstones of lacustrine facies with interbedded thin gypsum layers (inset of Fig. 2b) are found at an elevation of ~620 m, which marks the maximum level of the paleolake highstand; an alluvium layer, few meters in thickness, overlies the lacustrine facies. Stratigraphic evidence of a paleoshoreline at ~620 m was also found at the southern margin of the Sangequan block (site β, Fig. 2c). A deeply incised section exposes the stratigraphic sequence, revealing more than 20 m of yellowish mudstones, with occasional interbedded thin gypsum layers (inset of Fig. 2c), suggesting a former lacustrine environment; a thin alluvium layer overlies the lacustrine segment. Another lacustrine outcrop (Site γ, Fig. 2d) is at the southern edge of the Huanghuagou alluvial platform (*PL-HHG*), with the top of lacustrine facies at an altitude of 600 m under several meters of alluvial sediments. The presumed extent of the paleolake at its highstand stage is outlined by the 620-m contour (Fig. 2e).

3.2 Chronology

To constrain the chronosequence of the Irtysh River's evolution, we dated the alluvial deposits using a combination of cosmogenic ^{21}Ne exposure dating and $^{26}Al/^{10}Be$ burial dating. Surface ^{21}Ne concentrations provide minimal exposure ages of the landscape surface or maximal rates for regional erosion (Lal, 1991); for long-timescale exposure history, surface exposure age can be determined only when regional erosion is well-constrained. The development of isochron $^{26}Al/^{10}Be$ burial dating technique (Balco & Rovey, 2008) provides an effective way to accurately determine the burial ages of fluvial sediments that were shallowly buried (e.g., Erlanger et al., 2012; Odom, 2020).

Several alluvial platforms with areas greater than 200 km^2 are preserved in this region besides *PL-HHG*: *PL-JL* near the Jili Lake, *PL-KL* near the Kelang River, and *PL-TES* near Tieersihabahe (Fig. 2a). The former three sit within the extent the paleolake occupied, while *PL-TES*, as an alluvial fan that had drained into the paleolake, is beyond the presumed paleolake's scope and separated into two parts by a dry valley that eroded into the Paleozoic basement (Fig. 2a).

Depth profiles from alluvial sediments on platforms *PL-HHG*, *PL-JL*, and *PL-TES* were used for cosmogenic ^{21}Ne exposure dating. Depending on the sedimentary features (uniform or multistage deposition), subsurface samples were collected at regular intervals from the landscape surface to depths of 180–400 cm to constrain the inherited ^{21}Ne components. Downward-decreasing ^{21}Ne concentrations are expected in geomorphically stable alluvium; increasing nuclide concentrations with depth reveal an accumulating surface experiencing continuous deposition

(Phillips et al., 1998). Granite samples were collected from the surface of the Paleozoic granite bedrock on *PL-TES*.

Cosmogenic $^{26}Al/^{10}Be$ isochron burial dating was used at the site of platform *PL-KL*, where a roadcut exposes a ~6.5-m thick fluvial pebble bed, to constrain its depositional time. A series of quartzite gravel samples were collected horizontally at the bottom of the fluvial facies to ensure the same burial history.

Site descriptions are presented in Table 1. Sampling strategies and dating methods are described in the supplementary text and relevant figures, with the dataset listed in Suppl. Tables S1–2.

4 Results

The modeled ages of each platform are summarized in Table 1. On platforms *PL-HHG* and *PL-JL*, the uniform sedimentary facies of fluvial clasts exhibited exponentially decreasing ^{21}Ne concentrations with depth (Figs. 3a,b) and have respective minimum exposure ages of 1.56 ± 0.16 Ma and 2.39 ± 0.06 Ma, revealing an eroding regime that began no later than 2.4–1.6 Ma.

The sedimentary features of the alluvial fan *PL-TES* are clearly different from those of *PL-HHG* and *PL-JL*. Under a ~50-cm thick layer of capping soil, a thin segment of consolidated clasts (Unit 2, ~1.4 m) overlay the layer of silt sand (Unit 1), and a light-colored horizon of calcareous cement intercalated the two facies (Fig. 3c). The ^{21}Ne concentration profile showed a two-stage depositional sequence, consistent with the stratigraphy observed in the field (Fig. 3d). Taking the shielding effects of soil into account, the clast segment yielded a minimum age of 1.31 ± 0.34 Ma, revealing the diversion of the river to flowing northwest no later than 1.3 Ma. Paleozoic granite bedrock exposed in the dry valley yields a 1σ synchronous minimum age of 1.16 ± 0.04 Ma.

On platform *PL-KL*, the five samples yielded a $^{26}Al/^{10}Be$ burial isochron (Figs. 3e,f), corresponding to a burial age of 2.77 $^{+0.39}/_{-0.33}$ Ma for the overlying sand-pebble fluvial facies. The transition of sedimentary facies from underlying sandy suite to fluvial pebbles (Fig. 3e) reveals a significant hydrodynamic change, the age of which could be constrained to no later than $2.77^{+0.39}/_{-0.33}$ Ma, using the depositional age of the overlying segment. Furthermore, the increasing trend of ^{21}Ne concentration in the sandy suite with depth (Fig. 3g) uncovers continuous aggradation (Phillips et al., 1998) that ended during the late Pliocene in the Junggar.

To summarize, the results given above demonstrate that (1) the minimum ages of relict alluvial sediments within the Junggar Basin are potentially contemporaneous, ranging from late Pliocene (ca. 2.8 Ma) to Pleistocene (> 2.4–1.6 Ma); and (2) aggradation occurred in the Junggar Basin before 2.8 Ma, followed by a transition to an erosional regime before 2.4 Ma but no later than 1.6 Ma. This reveals the bursting of the Junggar paleolake in the late Pliocene, when global climate cooling culminated (Jansen et al., 1988; Ruddiman & Raymo, 1988; Shackleton et al., 1984).

5 Late-Pliocene birth of Irtysh River

Based on the chronological constraints and field evidence, we present a model for the evolution of the Irtysh River during the late Pliocene–Pleistocene period. After the late-Neogene tectonic rejuvenation of the Altay Mountains and the Mongolian plateau where major Siberian rivers originate (Fig. 1a), the topography of central Asia, which favors the formation of northward-flowing river systems, was shaped. Based on this tectonic prerequisite, a northwest-flowing trunk stream was established in the Junggar Basin, with other Altay-draining rivers flowing southward into this trunk stream, which then, drained into a lowland paleolake (Fig. 4a).

This drainage pattern lasted until ca. 2.8 Ma, and based on the altitudes of the localities portraying distinct evidences of lacustrine deposits, a united paleolake that occupied most of the Junggar Basin existed when the filling of the paleolake culminated (Fig. 4b). All regional river systems that flowed from the surrounding uplands probably drained into this paleolake. The storage of this paleolake was more than 8000 km^3 at its highstand stage, based on the thickness of lacustrine deposits, which is more than twice the annual water discharge of current Arctic rivers (3300 km^3/a) (Stein, 2000).

The increasing water level of this paleolake then cut through the lake barrier at the northern end of the Zaysan Basin and spilled downstream (Fig. 4b), initiating a fluvial incision and triggering the formation of the course of the Irtysh River. The water-spillover event coincides with the major episode of climate cooling and sea ice expansion during the late Pliocene deduced from globally distributed marine $\delta^{18}O$ records (Lisiecki & Raymo, 2005). The intensive terrestrial glaciation development and increased moisture delivery during the late Pliocene, as observed in the preserved records in Lake Baikal (Fig. 1b), brought increased flux of freshwater supply, and the significant drop in global base level at that time may have triggered the downcutting and, thus, the draining of the Junggar paleolake. The ancestral rivers from the Altay Mountains were reorganized into the northwest-flowing Irtysh River no later than the early Pleistocene (> 2.4–1.6 Ma); it cut through the Zaysan Valley, which then, became the pathway of the Irtysh River to flow northward (Fig. 4c).

6 Implication for Siberian-Arctic river system

Previous stratigraphic, geochemical, and geomorphological studies have pointed to a late-Pliocene age for the Siberian-Arctic river system. The chronological results obtained herein have constrained the initial establishment of the upper Irtysh River to the late Pliocene–early Pleistocene period. As a major Siberian river, the age of the Irtysh's establishment is consistent with previous results, and has added quantitative chronological evidence to the geologically estimated age of the Siberian-Arctic river system.

The temporal coincidence of the Siberian-Arctic river formation with the late-Pliocene ice advance in the Northern Hemisphere is striking; notably, the profound impact of Siberian freshwater input on the ice-sheet expansions also depends on the freshwater discharge rate. The bursting of the Junggar paleolake, which stored more than 8000 km^3 of water, would discharge into the Kara Sea (Fig. 1a) over a short period through the newly formed Irtysh River and provided the Arctic Ocean with more than twice the freshwater discharge of current Arctic rivers annually (3300 km^3/a).

The freshwater input to the Kara Sea would have been equivalent to an ~9-m layer of freshwater over its surface; according to the hydrographic data (Hanzlick & Aagaard, 1980), the average equivalent thickness of freshwater over the modern Kara Sea is approximately 3.5 m. Thus, the abrupt freshwater discharge of 8000 km^3 into the Kara Sea at the time would have significantly diminished the surface layer salinity, broken the vertical stability, and resulted in stronger stratification of the vertical circulation that favored sea ice formation, enhanced export of water and ice from the Arctic to Atlantic, thereby influenced global thermohaline circulation. These significant alterations would change the Arctic Ocean's mass and energy budgets, such as Earth's surface albedo, water vapor, heat and energy exchange between ocean and atmosphere, which have strong influences not only on the Arctic but also on the global climate system (Stein, 2000). A distinct climatic deterioration in the Arctic around 2.6 Ma has been recorded in Lake El'gygytgyn (Melles et al., 2012), which is a benchmark for understanding the pan-Arctic climate.

Notably, the Junggar paleolake was likely just one of several reservoirs in Siberia that could have provided huge pulses of freshwater runoff to the Arctic Ocean when the Siberian-Arctic river formed. Previous stratigraphic investigations on the western Siberian Plain (WSP, Fig. 1a) (Gnibidenko, 2007; Pospelova et al., 1977; Volkova, 2011) showed that during the late Neogene, lacustrine basins had developed in most areas of the southern part of WSP as the result of west-tilting paleotopography of Asia at the time (Wang, 2004). Estimates based on the extent to which the late-Neogene lacustrine deposits occupied and a shallowest thickness of ~5 m (Pospelova et al., 1977) suggest an additional freshwater storage of at least 4000 km^3 in WSP (Figure S5). Besides, after the Siberian rivers began to discharge into the Arctic, the increase in Eurasian moisture, transported by the westerlies since the early Pliocene, would also have enhanced freshwater delivery to the Arctic via the Siberian river system.

In conclusion, the coincidence of Arctic river formation in Siberia and the huge pulses of their runoff supports the profound impact of Siberian freshwater input on the late-Pliocene ice-sheet expansions in the Northern Hemisphere, which further affected global oceanographic and climatic systems.

Acknowledgments

This work was jointly supported by Grants-in-Aid from State Key Laboratory of Earthquake Dynamics (Grant No. LED2017A05), basic scientific research fund, Institute of Geology, China Earthquake Administration (Grant No. IGCEA1817), National Natural Science Foundation of China (Grant No. 41888101), and Second Tibetan Plateau Scientific Expedition and Research program (Grant No. 2019QZKK0704). Professional suggestions from Dr. William Odom and an anonymous reviewer helped us improve the manuscript. The authors declare that they have no conflict of interest. Datasets for this research are available in the repository: https://figshare.com/articles/dataset/_/14724438 (DOI:10.6084/m9.figshare.14724438.v1)

References

Aagaard, K., & Carmack, E. C. (1989). The role of sea ice and other fresh water in the Arctic circulation. *Journal of Geophysical Research Oceans, 94*(C10), 14485-14498. doi: 10.1029/JC094iC10p14485

Alekseev, M. N., & Drouchite, V. A. (2004). Quaternary fluvial sediments in the Russian Arctic and Subarctic: Late Cenozoic development of the Lena River system, northeastern Siberia. *Proceedings of the Geologists Association, 115*(4), 339-346. doi: 10.1016/S0016-7878(04)80013-0

Antipina, V., Afoninaa, T., Badalovb, O., Bezrukovac, E., Bukharovd, A., Bychinskya, V., et al. (2001). The new BDP-98 600-m drill core form Lake Baikal: a key late Cenozoic sedimentary section in continental Asia. *Quaternary International, 80-81*, 19-36. doi: 10.1016/S1040-6182(01)00016-7

Backman, J., Jakobsson, M., Frank, M., Sangiorgi, F., Brinkhuis, H., Stickley, C., et al. (2008). Age model and core-seismic integration for the Cenozoic Arctic Coring Expedition sediments from the Lomonosov Ridge. *Paleoceanography, 23*(1), PA1S03. doi: 10.1029/2007pa001476

Balco, G., & Rovey, C. W. (2008). An isochron method for cosmogenic-nuclide dating of buried soils and sediments. *American Journal of Science, 308*(10), 1083-1114. doi: 10.2475/10.2008.02

Balco, G., Stone, J. O., Lifton, N. A., & Dunai, T. J. (2008). A complete and easily accessible means of calculating surface exposure ages or erosion rates from ^{10}Be and ^{26}Al measurements. *Quaternary Geochronology, 3*(3), 174-195. doi: 10.1016/j.quageo.2007.12.001

Braucher, R., Merchel, S., Borgomano, J., & Bourlès, D. (2011). Production of cosmogenic radionuclides at great depth: a multi element approach. *Earth and Planetary Science Letters, 309*(1), 1-9. doi: 10.1016/j.epsl.2011.06.036

Caves, J. K., Winnick, M. J., Graham, S. A., Sjostrom, D. J., Mulch, A., & Chamberlain, C. P. (2015). Role of the westerlies in Central Asia climate over the Cenozoic. *Earth and Planetary Science Letters, 428*, 33-43. doi: 10.1016/j.epsl.2015.07.023

Codilean, A. T., Bishop, P., Stuart, F. M., Hoey, T. B., Fabel, D., & Freeman, S. P. (2008). Single-grain cosmogenic ^{21}Ne concentrations in fluvial sediments reveal spatially variable erosion rates. *Geology, 36*(2), 159-162. doi: 10.1130/g24360a.1

De Grave, J., & van den Haute, P. (2002). Denudation and cooling of the Lake Teletskoye Region in the Altai Mountains (South Siberia) as revealed by apatite fission-track thermochronology. *Tectonophysics, 349*, 145-159. doi: 10.1016/j.jseaes.2006.03.001

Eberhardt, P., Eugster, O., & Marti, K. (1965). A Redetermination of the Isotopic Composition of Atmospheric Neon. *Zeitschrift für Naturforschung A, 20*(4), 623-624. doi: 10.1515/zna-1965-0420

Erlanger, E. D., Granger, D. E., & Gibbon, R. J. (2012). Rock uplift rates in South Africa from isochron burial dating of fluvial and marine terraces. *Geology, 40*(11), 1019-1022. doi: 10.1130/g33172.1

Gnibidenko, Z. N. (2007). Late Cenozoic paleomagnetism of West Siberian Plate. *Russian Geology and Geophysics, 48*(4), 337-348. doi: 10.1016/j.rgg.2006.03.002

Gordeev, V. V., Martin, J. M., Sidorov, I. S., & Sidorova, M. V. (1996). A reassessment of the Eurasian river input of water, sediment, major elements, and nutrients to the Arctic Ocean. *American Journal of Science, 296*(6), 664-691. doi: 10.2475/ajs.296.6.664

Gordeev, V. V., Rachold, V., & Vlasova, I. E. (2004). Geochemical behaviour of major and trace elements in suspended particulate material of the Irtysh river, the main tributary of the Ob river, Siberia. *Applied Geochemistry, 19*(4), 593-610. doi: 10.1016/j.apgeochem.2003.08.004

Gosse, J. C., & Phillips, F. M. (2001). Terrestrial in situ cosmogenic nuclides: theory and application. *Quaternary Science Reviews, 20*(14), 1475-1560. doi: 10.1016/S0277-3791(00)00171-2

Guo, Z. T., Ruddiman, W. F., Hao, Q. Z., Wu, H. B., Qiao, Y. S., Zhu, R. X., et al. (2002). Onset of Asian desertification by 22 Myr ago inferred from loess deposits in China. *Nature, 416*(6877), 159-163. doi: 10.1038/416159a

Haley, B. A., Frank, M., Spielhagen, R. F., & Eisenhauer, A. (2007). Influence of brine formation on Arctic Ocean circulation over the past 15 million years. *Nature Geoscience, 1*(1), 68-72. doi: 10.1038/ngeo.2007.5

Hanzlick, D., & Aagaard, K. (1980). Freshwater and Atlantic water in the Kara Sea. *Journal of Geophysical Research Oceans, 85*(C9), 4937-4942. doi: doi.org/10.1029/JC085iC09p04937

Haug, G. H., Tiedemann, R., Zahn, R., & Ravelo, A. C. (2001). Role of Panama uplift on oceanic freshwater balance. *Geology, 29*(3), 207-210. doi: 10.1130/0091-7613(2001)029

Huang, F., Xia, Z., Li, F., Guo, L., & Yang, F. (2012). Hydrological changes of the Irtysh River and the possible causes. *Water resources management, 26*(11), 3159-3208. doi: 10.1007/s11269-012-0067-4

Jansen, E., Bleil, U., Henrich, R., Kringstad, L., & Slettemark, B. (1988). Paleoenvironmental changes in the Norwegian Sea and the northeast Atlantic during the last 2.8 m.y.: Deep

Sea Drilling Project/Ocean Drilling Program Sites 610, 642, 643 and 644. *Paleoceanography, 3*(5), 563-581. doi: 10.1029/pa003i005p00563

Jolivet, M., De Boisgrollier, T., Petit, C., Fournier, M., Sankov, V. A., Ringenbach, J. C., et al. (2009). How old is the Baikal Rift Zone? Insight from apatite fission track thermochronology. *Tectonics, 28*(3), TC3008. doi: 10.1029/2008tc002404

Klinger, Y., Etchebes, M., Tapponnier, P., & Narteau, C. (2011). Characteristic slip for five great earthquakes along the Fuyun fault in China. *Nature Geoscience, 4*(6), 389-392. doi: 10.1038/ngeo1158

Kohl, C. P., & Nishiizumi, K. (1992). Chemical isolation of quartz for measurement of in-situ-produced cosmogenic nuclides. *Geochimica et Cosmochimica Acta, 56*(9), 3583-3587. doi: 10.1016/0016-7037(92)90401-4

Knies, J., Cabedo-Sanz, P., Belt, S. T., Baranwal, S., Fietz, S., & Rosell-Mele, A. (2014). The emergence of modern sea ice cover in the Arctic Ocean. [Research Support, Non-U.S. Gov't]. *Nature communications, 5*, 5608. doi: 10.1038/ncomms6608

Kuzmin, M. I., Karabanov, E. B., Prokopenko, A. A., Gelety, V. F., Antipin, V. S., Williams, D. F., & Gvozdkov, A. N. (2000). Sedimentation processes and new age constraints on rifting stages in Lake Baikal: results of deep-water drilling. *International Journal of Earth Sciences, 89*, 183-192. doi: 10.1007/s005310000090

Kuzmin, M. I., Yarmolyuk, V. V., Karabanov, E. B., Kawai, T., Prokopenko, A. A., Bychinskyi, V. A., et al. (2003). Paleoclimate records from the Lake Baikal sediments and lava formations of the south Baikal volcanic area. In K. Kashiwaya (Ed.), *Long Continental Records from Lake Baikal* (pp. 23-41). Tokyo: Springer-Verlag. doi: 10.1007/978-4-431-67859-5_2

Lal, D. (1991). Cosmic ray labeling of erosion surfaces: in situ nuclide production rates and erosion models. *Earth and Planetary Science Letters*, *104*(2-4), 424-439. doi: 10.1016/0012-821X(91)90220-C

Li, C., Zheng, D., Sun, J., Yu, J., Ma, Y., Zhang, H., et al. (2020). Reconstruction on regional paleo-drainage evolution in the northern Junggar Basin, China during the last ~27 myr from provenance analyses and its implications for uplift of the Altai Mountains. *Palaeogeography, Palaeoclimatology, Palaeoecology, 537*, 109373. doi: 10.1016/j.palaeo.2019.109373

Lifton, N., Sato, T., & Dunai, T. J. (2014). Scaling in situ cosmogenic nuclide production rates using analytical approximations to atmospheric cosmic-ray fluxes. *Earth and Planetary Science Letters, 386*, 149-160. doi: 10.1016/j.epsl.2013.10.052

Lisiecki, L. E., & Raymo, M. E. (2005). A Pliocene-Pleistocene stack of 57 globally distributed benthic $\delta^{18}O$ records. *Paleoceanography, 20*(1), PA1003. doi: 10.1029/2004pa001071

Maslin, M. A., Li, X. S., Loutre, M. F., & Berger, A. (1998). The contribution of orbital forcing to the progressive intensification of northern hemisphere glaciation. *Quaternary Science Reviews, 17*(4–5), 411-426. doi: 10.1016/S0277-3791(97)00047-4

Ma, Y., Wu, Y., Li, D., & Zheng, D. (2015). Analytical procedure of neon measurements on GV 5400 noble gas mass spectrometer and its evaluation by quartz standard CREU-1. *International Journal of Mass Spectrometry, 380*, 26-33. doi: 10.1016/j.ijms.2015.03.004

Melles, M., Brigham-Grette, J., Minyuk, P. S., Nowaczyk, N. R., Wennrich, V., DeConto, R. M., et al. (2012). 2.8 million years of Arctic climate change from Lake El'gygytgyn, NE Russia. *Science, 337*(6092), 315-320. doi: 10.1126/science.1222135

Milanovsky, E. E. (2008). Origin and development of ideas on Pliocene and Quaternary glaciations in northern and eastern Europe, Iceland, Caucasus and Siberia. *Geological Society London Special Publications, 301*(1), 87-115. doi: 10.1144/SP301.6

Moran, K., Backman, J., Brinkhuis, H., Clemens, S. C., Cronin, T., Dickens, G. R., et al. (2006). The Cenozoic palaeoenvironment of the Arctic Ocean. *Nature, 441*(7093), 601-605. doi: 10.1038/nature04800

Niedermann, S., Graf, T., & Marti, K. (1993). Mass spectrometric identification of cosmic-ray-produced neon in terrestrial rocks with multiple neon components. *Earth and Planetary Science Letters, 118*(1), 65-73. doi: 10.1016/0012-821x(93)90159-7

Nishiizumi, K. (2004). Preparation of ^{26}Al AMS standards. *Nuclear Instruments and Methods in Physics Research B, S223–224*, 388-392. doi: 10.1016/j.nimb.2004.04.075

Nishiizumi, K., Imamura, M., Caffee, M. W., Southon, J. R., Finkel, R. C., & Mcaninch, J. (2007). Absolute calibration of Be-10 AMS standards. *Nuclear Instruments and Methods in Physics Research Section B: Beam Interactions with Materials and Atoms, 258*, 403-413. doi: 10.1016/j.nimb.2007.01.297

Norris, T. L., Gancarz, A. J., Rokop, D. J., & Thomas, K. W. (1983). Half-life of ^{26}Al. *Journal of Geophysical Research: Solid Earth, 88*(S01), B331–B333. doi: 10.1029/JB088iS01p0B331

Odom, W. E. (2020). Dating the Cenozoic incision history of the Tennessee and Shenandoah Rivers with cosmogenic nuclides and ^{40}Ar/^{39}Ar in manganese oxides, (Doctor of Philosophy). Purdue University, West Lafayette, IN, US.

Perg, L. A., Anderson, R. S., & Finkel, R. C. (2001). Use of a new ^{10}Be and ^{26}Al inventory method to date marine terraces, Santa Cruz, California, USA. *Geology, 29*(10), 879-882. doi: 10.1130/0091-7613(2001)0292.0

Phillips, W. M., McDonald, E. V., Reneau, S. L., & Poths, J. (1998). Dating soils and alluvium with cosmogenic ^{21}Ne depth profiles: case studies from the Pajarito Plateau, New Mexico, USA. *Earth and Planetary Science Letters, 160*(1), 209-223. doi: 10.1016/s0012-821x(98)00076-4

Pospelova, G. A., Gnibidenko, Z. N., & Adamenko, O. M. (1977). A Neogene-Quaternary magnetic-biostratigraphic reference section in the south of Western Siberia. *International Geology Review, 19*(9), 1065-1076. doi: 10.1080/00206817709471108

Raymo, M. E., & Ruddiman, W. F. (1992). Tectonic forcing of late Cenozoic climate. *Nature, 359*, 117-122. doi: 10.1038/359117a0

Raymo, M. E., Ruddiman, W. F., & Froelich, P. N. (1988). Influence of late Cenozoic mountain building on ocean geochemical cycles. *Geology, 16*(7), 649-653. doi: 10.1130/0091-7613(1988)016

Ruddiman, W. F., & Raymo, M. E. (1988). Northern Hemisphere Climate Regimes During the Past 3 Ma: Possible Tectonic Connections. *Philosophical Transactions of the Royal Society B, 318*, 411-429. doi: 10.1098/rstb.1988.0017

Shackleton, N. J., Backman, J., Zimmerman, H., Kent, D. V., Hall, M. A., Roberts, D. G., et al. (1984). Oxygen isotope calibration of the onset of ice-rafting and history of glaciation in the North Atlantic. *Nature, 307*(5952), 620-623. doi: 10.1038/307620a0

Sharma, M., Basu, A. R., & Nesterenko, G. V. (1991). Nd-Sr isotopes, petrochemistry, and origin of the Siberian flood basalts, USSR. *Geochimica et Cosmochimica Acta, 55*, 1183-1192. doi: 10.1016/0016-7037(91)90177-7

Stein, R. (2000). Circum-Arctic river discharge and its geological record: an introduction. *International Journal of Earth Sciences*, *89*(3), 447-449. doi: 10.1007/s005310000110

Sun, J., Ye, J., Wu, W., Ni, X., Bi, S., Zhang, Z., et al. (2010). Late Oligocene-Miocene mid-latitude aridification and wind patterns in the Asian interior. *Geology, 38*(6), 515-518. doi: 10.1130/G30776.1

Tian, L., Masson-Delmotte, V., Stievenard, M., Yao, T., & Jouzel, J. (2001). Tibetan Plateau summer monsoon northward extent revealed by measurements of water stable isotopes. *Journal of Geophysical Research Atmospheres*, *106*(D22), 28081-28088. doi: 10.1029/2001JD900186

Tiedemann, R., Sarnthein, M., & Shackleton, N. J. (1994). Astronomic timescale for the Pliocene Atlantic $\delta^{18}O$ and dust flux records of Ocean Drilling Program site 659. *Paleoceanography, 9*(4), 619-638. doi: 10.1029/94PA00208

Vassallo, R., Jolivet, M., Ritz, J. F., Braucher, R., Larroque, C., Sue, C., et al. (2007). Uplift age and rates of the Gurvan Bogd system (Gobi-Altay) by apatite fission track analysis. *Earth and Planetary Science Letters, 259*(3-4), 333-346. doi: 10.1016/j.epsl.2007.04.047

Vermeesch, P., Balco, G., Blard, P.-H., Dunai, T. J., Kober, F., Niedermann, S., et al. (2015). Interlaboratory comparison of cosmogenic ^{21}Ne in quartz. *Quaternary Geochronology, 26*, 20-28. doi: 10.1016/j.quageo.2012.11.009

Volkova, V. S. (2011). Paleogene and Neogene stratigraphy and paleotemperature trend of West Siberia (from palynologic data). *Russian Geology and Geophysics, 52*(7), 709-716. doi: 10.1016/j.rgg.2011.06.003

Vorobyova, G. A., Mats, V. D., & Shimaraeva, M. K. (1995). Late-Cenozoic paleoclimates in the Baikal region. *Russian Geology and Geophysics, 36*, 82-96.

Wagner, T., Fabel, D., Fiebig, M., Häuselmann, P., Sahy, D., Xu, S., & Stüwe, K. (2010). Young uplift in the non-glaciated parts of the Eastern Alps. *Earth and Planetary Science Letters, 295*(1–2), 159-169. doi: 10.1016/j.epsl.2010.03.034

Wang, P. (1990). Neogene stratigraphy and paleoenvironments of China. *Palaeogeography Palaeoclimatology Palaeoecology, 77*(3-4), 315-334. doi: 10.1016/0031-0182(90)90183-8

Wang, P. (2004). Cenozoic Deformation and History of Sea-Land Interactions in Asia. *Earth Science-Journal of China University of Geosciences, 149*(1), 1-21. doi: 10.1029/149GM01

Williams, D. F., Peck, J., Karabanov, E. B., Prokopenko, A. A., Kravchinsky, V., King, J., & Kuzmin, M. I. (1997). Lake Baikal record of continental climate response to orbital insolation during the past 5 million years. *Science, 278*, 1114-1117. doi: 10.1126/science.278.5340.1114

Xu, Q. Q., Ji, J. Q., Sun, D. X., & Zhao, L. (2015). Late Cenozoic uplift-exhumation history of Qinghe-Fuyun region, Altay, Xinjiang-Evidence from apatite fission track. *Geological Bulletin of China, 34*(5), 834-845.

Yan, Q. S., & Xia, X. C. (1962). Geomorphological development in the source region of Irthsh and Ulungur Rivers in northern Xinjiang Province. *Acta Geographica Sinica*, *28*(4), 257-274.

Yuan, W., Carter, A., Dong, J., Bao, Z., An, Y., & Guo, Z. (2006). Mesozoic-Tertiary exhumation history of the Altai Mountains, northern Xinjiang, China: New constraints from apatite fission track data *Tectonophysics, 412*(3-4), 183-193. doi: 10.1016/j.tecto.2005.09.007

Zachos, J., Pagani, M., Sloan, L., Thomas, E., & Billups, K. (2001). Trends, rhythms, and aberrations in global climate 65 Ma to present. *Science*, *292*(5517), 686-693. doi: 10.1126/science.1059412

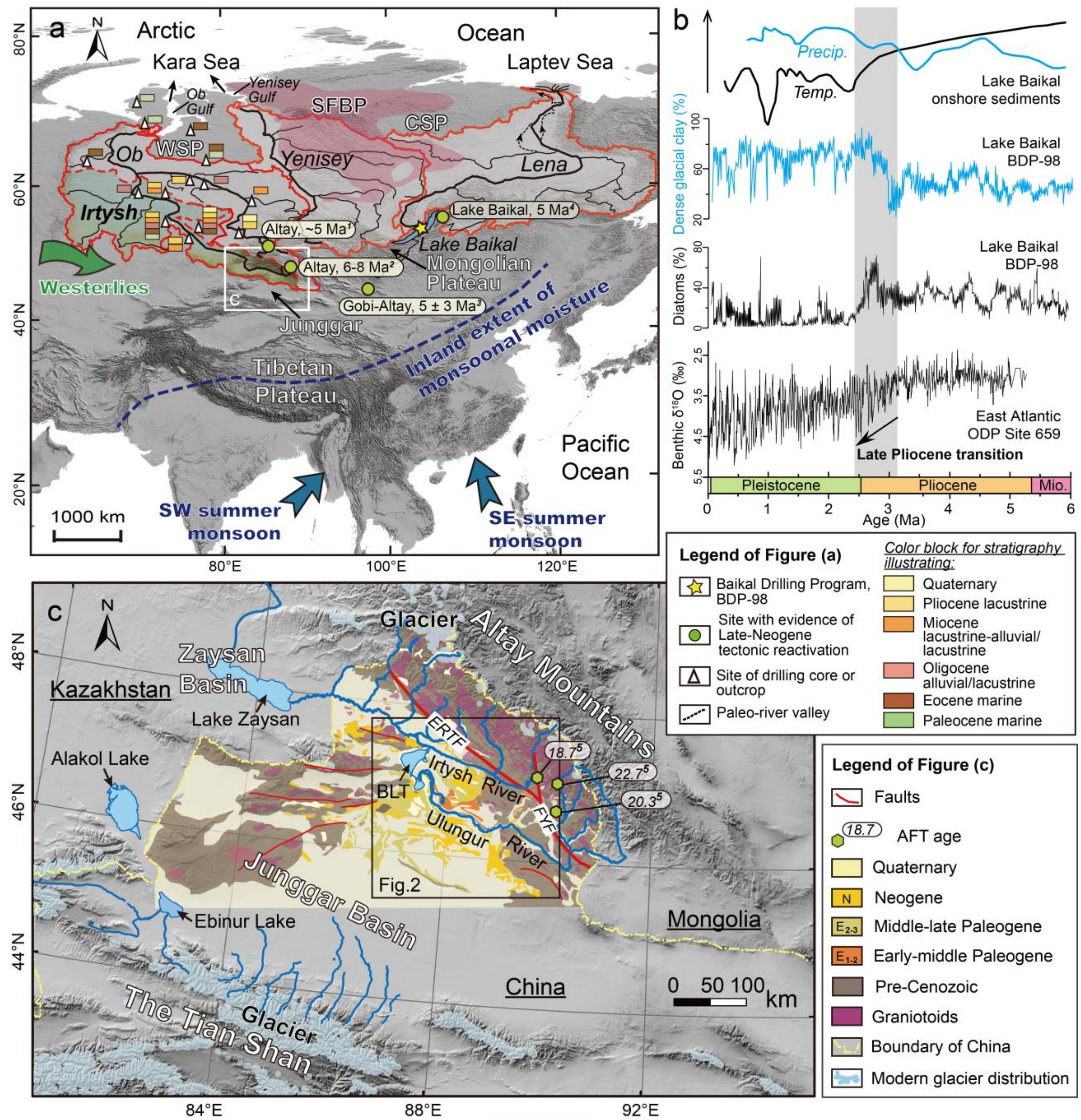

Figure 1. Major Arctic rivers and geological setting in Siberia. (**a**) The Yenisey, Lena, and Ob Rivers are shown in black and their watershed boundaries in red. The region visualized with a color ramp within the Ob watershed indicates the Irtysh catchment. Study area is shown in white rectangle. WSP: West Siberian Plain; CSP: Central Siberian Platform; SFBP: Siberian Flood Basalts Province, outlined roughly by the light pink area (Sharma et al., 1991). Color block

sequence illustrates stratigraphy in WSP (Volkova, 2011 and references therein); thicknesses of color blocks are arbitrary. [1]De Grave and van den Haute (2002), [2]Xu et al. (2015), [3]Vassallo et al. (2007), [4]Jolivet et al. (2009). (**b**) Global and regional terrestrial paleoclimatic proxies for the past 6 Ma. From bottom to top, deep-sea oxygen records from ODP Site 659 in east Atlantic (Tiedemann et al., 1994); diatom abundance and dense glacial clay in sediments from Lake Baikal (BDP-98) (Kuzmin et al., 2003); pollen-based temperature and precipitation reconstructions from onshore sediments of Baikal (Antipina et al., 2001; Vorobyova et al., 1995). (**c**) Topographic and geologic maps of Junggar Basin. BLT: Buluntuo Lake; ERTF: Ertix fault; FTF: Fuyun fault. [5]Xu et al. (2015).

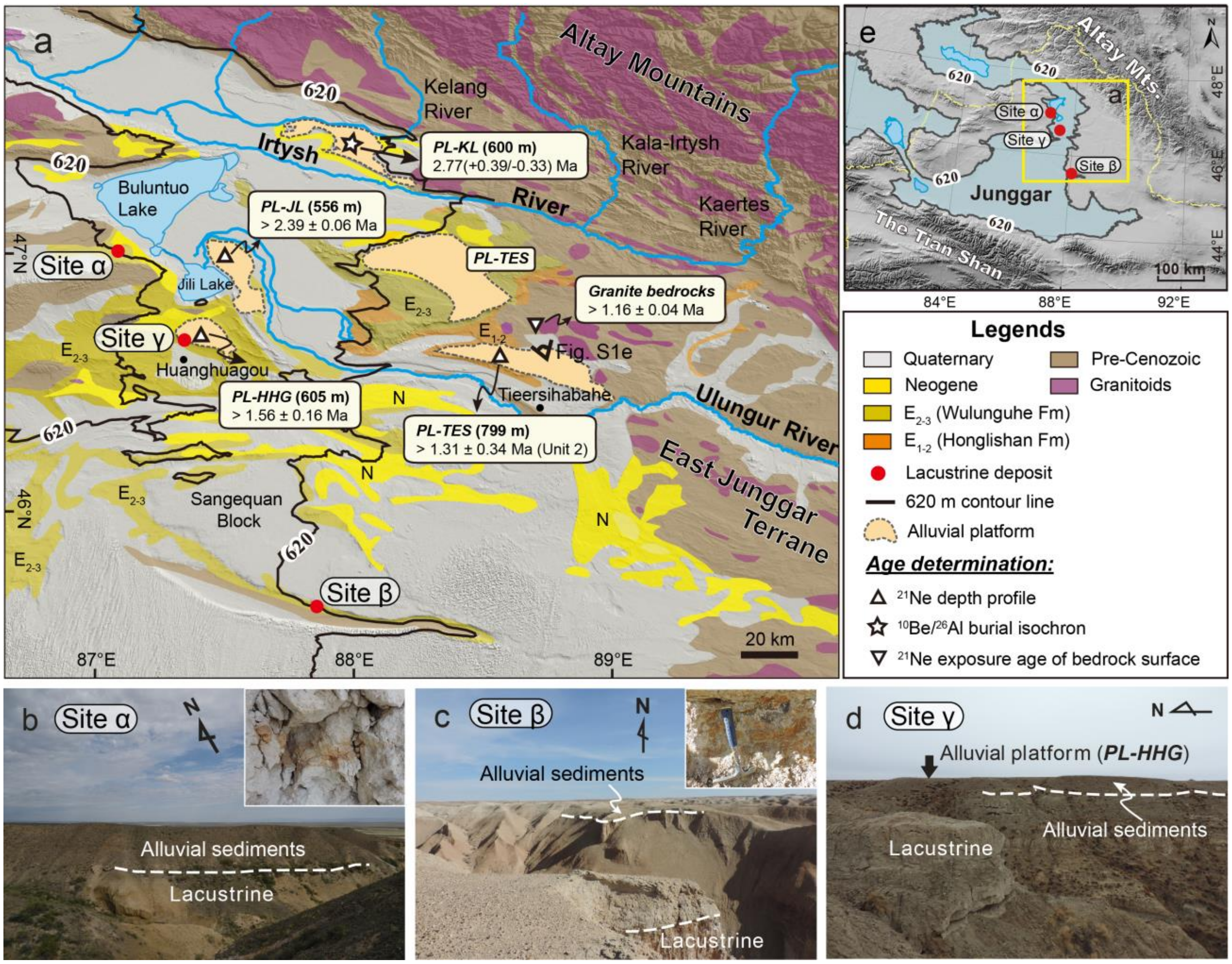

Figure 2. Pliocene lacustrine-alluvial remnants and geochronology (**a**). Red dot shows field sites with lacustrine evidence, with field image showing in (**b**)-(**d**) (inset: texture of calcite cements in lacustrine deposits). Triangle and star show sampling sites on alluvial platforms, with platform elevations and dating results shown in white rectangles. The black line is the presumed shoreline of paleolake at its highstand of 620 m, with the overview shown in (**e**). The paleolake's extent is visualized by light blue.

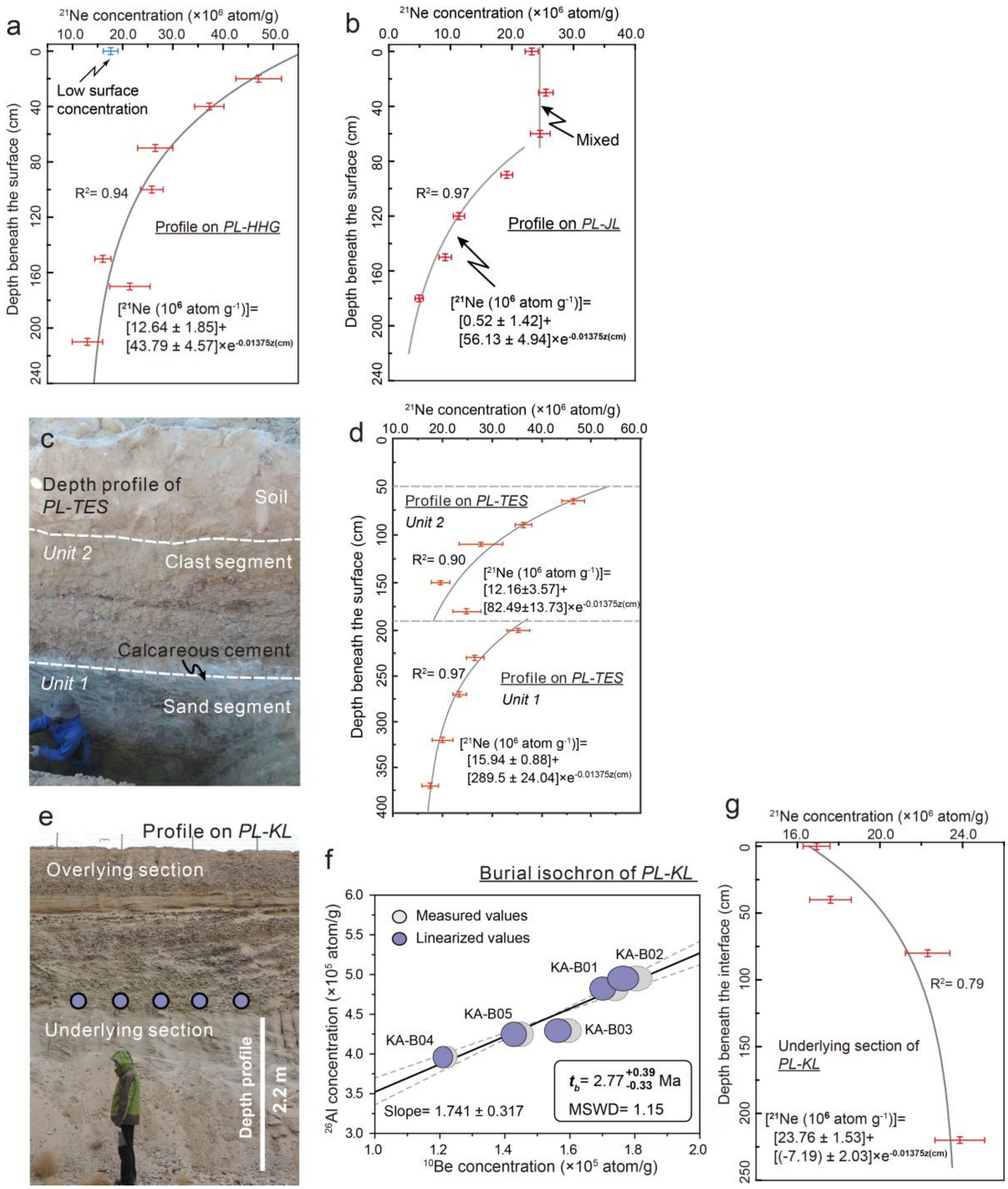

Figure 3. Chronology in Junggar Basin. (**a,b**) ^{21}Ne concentration profiles of *PL-HHG* and *PL-JL*, plotted against depth beneath platform surface. Error bars represent 1σ uncertainties. Blue datum point was not used in fitting. The grey line shows the best-fitted exponential function of ^{21}Ne concentration versus depth, and the asymptotic value represents inherited ^{21}Ne concentration in

sediments. (**c**) Field image of the hand-dug depth profile more than 4 m on *PL-TES*, and the ^{21}Ne concentration profile (**d**). (**e**) Field image of profile on *PL-KL* exposed along roadcut, and ^{26}Al/^{10}Be burial dating isochron of overlying section (**f**), with data shown as 1σ error ellipse for each sample and all samples used in regression, and ^{21}Ne concentration profile of underlying section (**g**).

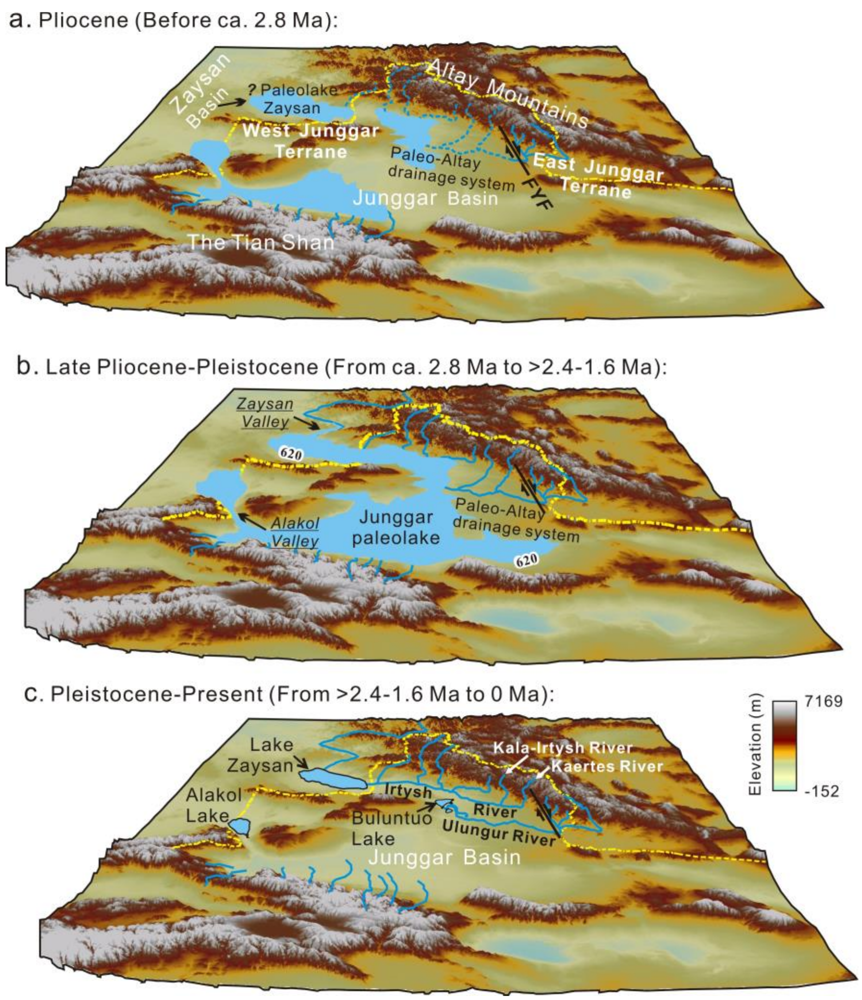

Figure 4. Simplified model of drainage system evolution in Junggar Basin. (**a**) Paleo-drainage system. Hypothetical river courses are shown as dotted lines. Light blue areas show the hypothetical lakes. (**b**) Onset of paleolake overflow and river system integration. Light blue

shading shows the area of the presumed Junggar paleolake at its highstand of 620 m. (**c**) Modern drainage system.

Table 1

Descriptions of the Platforms and Ages

Platform ID	Profile location	Elevation (m)	Sample type	Age type[a]	Age[b] (Ma)	Description
PL-HHG	46.6784°N 87.3918°E	605	Groups of clasts	^{21}Ne profile	>1.56 ± 0.16	Relict platform of alluvial deposits preserved in drainage basin occupied by the paleolake. Depth profile shows uniform sedimentary facies. Sampling pit is hand digging.
PL-KL	47.4089°N 88.0025°E	600	Groups of clasts	^{26}Al/^{10}Be burial isochron	2.77(+0.39/-0.33)	Relict platform of alluvial deposits preserved in drainage basin occupied by the paleolake. Sampling profile was exposed in the roadcut along Kui-A expressway, in which the overlying fluvial gravel layer showing bottom boundary on the underlying sand deposits.
PL-JL	47.0547°N 87.4628°E	556	Groups of clasts	^{21}Ne profile	>2.39 ± 0.06	Relict platform of alluvial deposits preserved in drainage basin occupied by the paleolake. Sampling profile was exposed in roadcut, showing uniform sedimentary facies.
PL-TES	46.6294°N 88.5623°E	799	Groups of clasts (Unit 2) Sand (Unit 1)	^{21}Ne profile	>1.31 ± 0.34 (Unit 2)	Alluvial fan at mountain front of Altay Mountain. Beyond the extent the paleolake occupied. Depth profile shows a multistage depositional sequence–a 50-cm-thick loose sediments, coarse gravel and fine sand deposited in the sedimentary sequence from top to bottom. Machine excavated trench.
Granite bedrock	46.7583°N 88.6353°E	695	Granite	^{21}Ne surface	>1.16 ± 0.04	Granite bedrock, protruding through the Paleozoic basements between two parts of fan *PL-TES*.

Note. Abandoned or depositional ages of the alluvial sediments and bedrocks.

[a]Abandoned ages of relict alluvial platform and surface exposure age of granite bedrock were determined by using ^{21}Ne exposure dating, and depositional age of *PL-KL* alluvial sediment was determined by using ^{26}Al/^{10}Be isochron burial dating. ^{21}Ne exposure dating gives the minimal exposure age for each platform.

[b]For age calculation, the production rate was calculated by CRONUS-Earth online calculator (Balco et al., 2008) using the time-dependent LSD production rate scaling model (Lifton et al., 2014). The ^{10}Be half-life of 1.36×10^6 a (Nishiizumi et al., 2007) and ^{26}Al half-life of 7.05×10^5 a (Nishiizumi, 2004; Norris et al., 1983) were used. The uncertainties of ages only include the analytical uncertainties. For platform *PL-TES*, the profile dug on the alluvial fan's surface consisted of two different sedimentary facies, and the abandonment age was calculated using the ^{21}Ne concentration profile of the upper clast layer.